J Radioanal Nucl Chem
DOI 10.1007/s10967-016-5164-z

Chelator-free radiolabeling of dextran with ^{68}Ga for PET studies

Nazila Gholipour[1] · Mehdi Akhlaghi[2] · Amin Mokhtari Kheirabadi[2] · Davood Beiki[2] · Parham Geramifar[2] · Hassan Yousefnia[3] · Mohammad Mazidi[3]

Received: 18 September 2016

Abstract The possibility of ^{68}Ga-dextran complex formation was analyzed in an HEPES-buffered (pH = 4.5) as well as in an alkaline (pH = 9) solution. The result outlined that the alkaline solution was more efficient to achieve a radiolabeling efficiency of 99% for a 5 mg ml^{-1} dextran solution (10 min, 90 °C). ^{68}Ga-dextran was stable 88, 71 and 86% after 2 h at storage and toward cysteine solution and human serum, respectively. The highest ROI derived %ID g^{-1} was found within the lungs, followed by the blood, liver, and bladder. Furthermore, a significant uptake was observed in the cartilage tissue. ^{68}Ga-dextran excreted more by the urinary and less by the biliary pathways.

Keywords Dextran · ^{68}Ga · PET/CT · ROI · Biodistribution

Introduction

Today, the availability of PET imaging systems around the world is dramatically increasing. PET represents more advantages over SPECT; such as high resolution and accuracy, short-time imaging protocols and lower radiation exposure to patients [1–3]. These advantages led to a major shift from SPECT to PET in several diagnosis protocols by the use of new PET tracers instead of the SPECT ones [4, 5]. This transition has offered new opportunities for researchers to focus on the production of new PET tracers.

The radionuclide angiography is a technique to assess regional blood volume using radioactive blood pool probes. The ^{99m}Tc-labeled red blood cells (^{99m}Tc-RBC) is a conventional radioactive probe for radionuclide angiography. However, Due to all associated risks on the blood handling, ^{99m}Tc-HSA, ^{99m}Tc-dextran [6] and ^{67}Ga-hyperbranched polyglycerols (^{67}Ga-HBGN) [7] were used as substitutes of ^{99m}Tc-RBC.

To benefit from the advantages of PET, several positron emitter blood-pool tracers, such as [^{15}O]CO–, [^{11}C]CO–labeled RBC, ^{62}Cu–, ^{18}F–, ^{68}Ga-HSA, and ^{68}Ga-HBGN have been introduced [7–11]. However, every tracer has limitations on its application. The use of radiolabeled RBC is limited due to blood handling problems and short half-lives of C-11 and O-15 radioisotopes (20.4 min for C-11 and 2.05 min for O-15) [8]. The use of ^{62}Cu-HSA is also limited because of the short half-life of Zn-62(9.2 h), the source of Cu-62 radioisotope in the ^{62}Zn/^{62}Cu generator [9, 10]. Fluorine-18 radiolabeling of HSA requires a pre-radiolabeled activated esters or aldehydes to be conjugated to the amine groups of HSA, where the whole process takes a long time [11]. Eventually, to prepare ^{68}Ga- HSA and ^{68}Ga-HBGN, the desired molecules must be conjugated to the suitable chelator in the first step [7, 8]. In the case of SPECT blood-pool radiotracers, ^{99m}Tc-dextran was preferred over ^{99m}Tc-HSA, due to its complete conformity of requirements such as straightforward and inexpensive labeling method, stability and remaining in the vascular space and providing minimal risk to the patient [6].

Although, dextran has been modified and be used to prepare radioligands such as ^{188}Re-cysteine dextran [12] for

Electronic supplementary material The online version of this article (doi:10.1007/s10967-016-5164-z) contains supplementary material, which is available to authorized users.

✉ Mehdi Akhlaghi
m-akhlaghi@sina.tums.ac.ir

[1] Faculty of Pharmacy, Baqiyatallah University of Medical Sciences, Tehran, Iran

[2] Research Center for Nuclear Medicine, Tehran University of Medical Sciences, Tehran, Iran

[3] Nuclear Science and Technology Research Institute (NSTRI), Tehran, Iran

Published online: 02 January 2017

radiotherapy, ^{99m}Tc-mannosylated cysteine dextran [13], ^{99m}Tc-DTPA-Mannosyl-dextran [14, 15] and ^{99m}Tc-MAG$_3$-mannosyl-dextran [16] for SPECT. However, several metal dextran complexes were successfully prepared by the direct interaction between dextran and metal ions such as Cu(II), Zn(II), Co(II), Mn(II), Ni(II), Ca(II), Fe(III), Tb(III) and Al(III) in neutral or alkaline solutions. The maximum metal ions interaction with dextran has been reported to be dependent on the pH and was at pH = 6–8 for Cd(II), Pb(II), Ca(II), Tb(III), Fe(III) and Al(III) and was at pH = 10–12 for Mn(II), Zn (II), Cu (II), Co(II) and Ni(II) [17–19]. The suitable pH for dextran complex formation depends on nature of metal ions. So that, by increasing the pH from neutral to alkaline, precipitation of some metal hydroxide complex, such as $Tb(OH)_3$, $Al(OH)_3$, $Pb(OH)_2$, strongly competes with dextran complex formation.

^{68}Gallium (^{68}Ga) is a generator-produced PET radionuclide which decays with a half-life of 67.83 min to the stable daughter isotope ^{68}Zn. The radioactive decay is accompanied by the positron annihilation results in two 511 keV gamma photons emitted in opposite directions suitable for positron emission tomography [20]. The availability of an approved pharmaceutical grade ^{68}Ge/^{68}Ga generator allows hospitals economical and routinely access to a PET isotope without expensive cyclotron facilities. For this reason, the number of publications dedicated to ^{68}Ga has increased drastically in the basic and clinical research during recent years [21–24].

Since, Ga(III) has a similar coordination chemistry of Fe(III), Tb(III) and Al(III) [25]. The simple and inexpensive preparation of chelator-free ^{68}Ga-dextran complex was the goal of this work. Furthermore, dextran has been used to prepare low toxic and water soluble dextran coated metal oxides nanoparticles [25–27]. The successful chelator-free radiolabeling of dextran could be a basis for chelator-free radiolabeling of dextran coated metal oxides nanoparticles for PET-MRI dual modality imaging. To prepare a high-yield ^{68}Ga-dextran complex, the effects of pH, temperature and reaction time on complex formation efficiency were investigated. The stability of prepared ^{68}Ga-dextran was evaluated in the storage solution as well as toward cysteine and serum solution. The radiocomplex was injected into the tail vein of healthy male rats, and the biodistribution was assessed by tissue sampling and ROI analysis.

Experimental

Materials and methods

Dextran (MW = 35–45 kDa) was purchased from Sigma. The ^{68}Ge/^{68}Ga generator (20 mCi/elution) was a gift from Pars Isotope Co. Karaj, Iran. The ^{68}Ge/^{68}Ga generator was eluted with 0.6 mol L^{-1} HCl solution to obtain an acidic solution of $^{68}GaCl_3$. All other chemicals were obtained from Merck. A digital hot-pot heater (Turkey) was used to heat vials at the defined temperature. A miniGita radio-TLC scanner equipped with Gina-star software, Raytest, Germany was used to plot TLC radiochromatograms.

^{68}Ge/^{68}Ga generator performance and quality control

^{68}Ge/^{68}Ga generator was eluted with 0.6 mol L^{-1} HCl solution, and 0.5 ml fractions were collected. The fractions 2–4, which had the highest radioactivities, were transferred to a 10 ml borosilicate pyrogen-free vial and checked for radiochemical purity according to the method, has been reported previously [28].

Radiolabeling of dextran

Two methods were applied for the direct radiolabeling of dextran; the first, radiolabeling in an acidic solution of $^{68}GaCl_3$ and the second, radiolabeling in an alkaline solution. For the first method, briefly, 550 MBq of $^{68}GaCl_3$ solution was transferred to a 10 ml borosilicate pyrogen-free vial and then 400 mg of HEPES was added to adjust the pH to 4.5. Subsequently, 0.5 ml of 5, 10, 20 and 40 mg ml^{-1} of dextran solutions were added to ^{68}Ga solutions, and the mixtures were kept at room temperature or were heated at 90 °C. The radiolabeling efficiencies were assessed by chromatography on TLC-SG, Merck, 105554 and, 10 mmol L^{-1} DTPA (pH = 5.5) solution as developing solution during the radiolabeling time. In this system, $^{68}Ga(OH)_3$ colloids, ^{68}Ga(III) (as DTPA complex) and labeled dextran have R_f values of 0.0, 0.8 and 0.4, respectively.

The latter, due to the similarity of the solution and coordination chemistries of Ga(III) ions to Fe(III) ions [29], the previously reported method for preparation of Fe-dextran complex was simulated to prepare ^{68}Ga-dextran complex in an alkaline solution [18] with a minor modification. Briefly, a series of dextran solutions of 5, 10, 20 and 40 mg ml^{-1} concentration was prepared and heated at 90 °C for 1 h with continuous agitation. In the following, 5 mol L^{-1} NaOH was added to the solutions to adjust the pH to 9 and then were heated for 10 min to accelerate deprotonation of dextran hydroxyl groups. Subsequently, 0.5 ml fractions of dextran alkaline solutions were added to ^{68}Ga solutions followed by the addition of 5 mol L^{-1} NaOH solution to adjust the pH to 9. The mixtures were kept at room temperature or heated at 90 °C, and the radiolabeling efficiencies were checked as described above (Fig. 1 in supplementary information). Finally, the pH was adjusted to 7 for subsequent stability assays and biodistribution studies.

Stability studies in storage solution and toward cysteine and human blood serum

The stability of the ^{68}Ga-dextran complex was assayed in the storage solution and toward cysteine and human blood serum. The complex solution (pH = 7) was kept at room temperature, and the radiochemical purity was checked in the interval up to 2 h likewise the method was described above.

A cysteine solution (10 mg ml^{-1}) was freshly prepared in 100 mmol L^{-1} phosphate buffer. To assay transchelation of ^{68}Ga from dextran to cysteine, 10 µl of the ^{68}Ga-dextran solution was mixed with 500 µl of cysteine solution and the mixture was incubated at 37 °C for 2 h. At defined intervals, 10 µl aliquots of the mixture were tested to determine radioactive fractions by thin layer chromatography on TLC-SG and methanol as mobile phases. In this system, ^{68}Ga-dextran, free ^{68}Ga and ^{68}Ga(OH)$_3$ have a R_f value of 0.0–0.3 and ^{68}Ga-cyteine migrates to $R_f = 0.6$ (Fig. 2 in supplementary information).

Stability of ^{68}Ga-dextran complex was also examined in the presence of fresh human serum by incubating the mixture of same volumes of them at 37 °C for 2 h at atmospheric conditions. At defined intervals, the radiochemical purity was checked on TLC-SG and normal saline as the mobile phase. In this system, the radiolabeled components of serum remain at the origin, while ^{68}Ga-dextran migrates to $R_f = 0.4$ (Fig. 3 in supplementary information).

Biodistribution studies

The biodistribution of ^{68}Ga-dextran among organs was determined in wild-type male rats, according to our previous work [28]. The animals were sacrificed by CO_2 asphyxiation at selected times after injection (n = 3 for each interval), and specific activities of tissues were determined as a percent of injected dose per gram of tissues.

PET–CT studies and data analysis

PET/CT imaging was performed by a clinical PET/CT scanner (Biograph 6 TrueX; Siemens Medical Solutions). The male rat was tail-vein injected with ~6.6 MBq (120 µCi) of ^{68}Ga-dextran under ketamine–xylazine anesthesia. Then, it was placed in a supine position on the PET/CT table, and CT scan was performed for anatomical reference and attenuation correction (spatial resolution 1.25 mm, 80 kV, 150 mAs, 20 s). Static PET images were acquired for 10 min with 4 sets of emission images starting 30, 60, 90 and 120 min after injection. Reconstruction was performed using the iterative algorithm with attenuation correction according to our previous work [28]. Using Siemens SyngoMMWP VE36A workstation, 3D ROIs were drawn manually on the coronal CT images for each major organ and a background ROI outside the body area, which were overlaid on the decay corrected static coronal PET image. To minimize the effects of accumulated radioactivity in the adjacent tissues, the size of each ROI was smaller than the actual size of each organ. The radioactivity concentrations (accumulation) within interested organs were obtained from average radioactivity concentration (Bq ml^{-1}) within the multiple-ROI volumes (Fig. 4 in supplementary information). The ROIs were converted to Bq g^{-1} by assuming the average densities of 0.26 and 1 g ml^{-1} for the lung and other organs, respectively [30]. Finally, the ROIs were divided by the administered radioactivity to obtain imaging ROI–derived percentage injected dose per gram of organs.

On the other hand, a 3D ROI was drawn around whole-body of rates for extracting whole-body volume and average radioactivity concentration, used to calculate the total accumulated radioactivity at each time of the study (Fig. 5 in supplementary information). To determine the uptake and release profiles of interested organs, the behavior in the ratios of the radioactivity concentration of organs to the total radioactivity at the time of studies was plotted.

Result and discussion

Quality control of $^{68}GaCl_3$

The elution efficiency of the ^{68}Ge/^{68}Ga generator was about 80%, and the fractions of 2–4 had the highest radioactivity around 90% of total eluted radioactivity. Figure 1 shows the radiochromatogram of the $^{68}GaCl_3$ solution. As can be seen from the Fig. 1, ^{68}Ga existed mostly as reactive ^{68}Ga(III) cation which has formed ^{68}Ga-DTPA chelate and migrated to $R_f = 0.8$.

Radiolabeling of dextran

^{68}Ga radioisotope is typically chelated at acidic pH to avoid the formation of Ga(OH)$_3$ solid precipitation. Figure 2 provides the effect of dextran concentration and reaction time on the radiolabeling efficiency in the acidic solution and at room temperature or 90 °C (method 1). As shown, there is a clear trend of increasing in the radiolabeling efficiency with concentration and reaction time. Furthermore, the heating showed an increasingly positive effect. Nevertheless, it reached up to 85% for maximum applied dextran concentration even after 60 min heating at 90 °C.

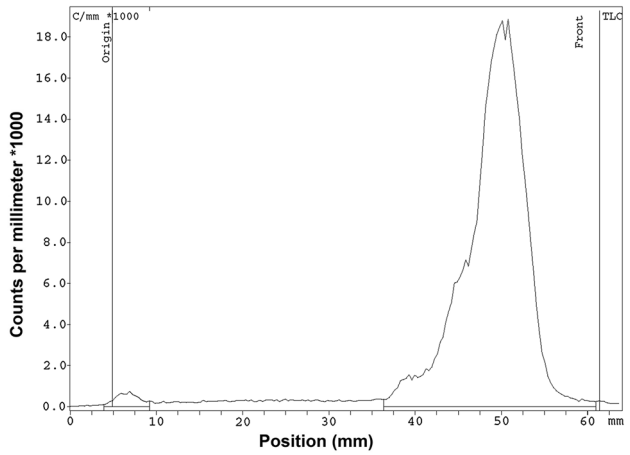

Fig. 1 Radiochromatogram of eluted $^{68}GaCl_3$ solutions on Whatman No 1 and 10 mM DTPA (pH = 5.5) solution as mobile phase

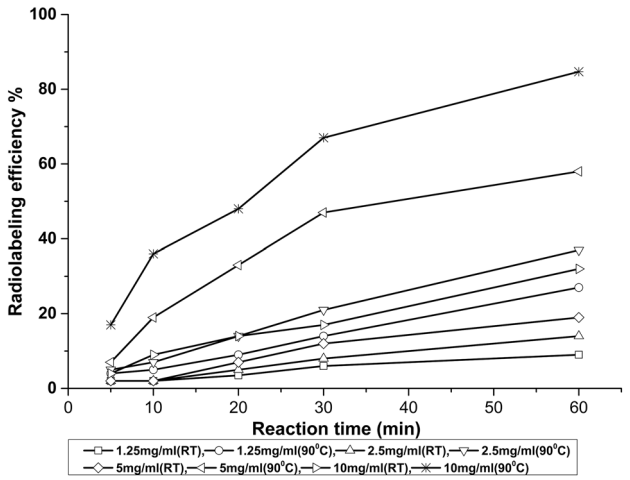

Fig. 2 Radiolabeling efficiency of dextran with ^{68}Ga in the acidic HEPES solution at room temperature and 90 °C (method 1). Each point represents the average of three independent tests

Despite the high tendency of gallium to form chelates through bonds with oxygen [29], the efficiency of gallium dextran complexes was low in the acidic pH, used routinely to prepare ^{68}Ga radio-complexes. To increase the probability of forming a ^{68}Ga-dextran complex, the hydroxyl groups of dextran were deprotonated in alkaline solution. Figure 3 presents the effect of dextran concentration and reaction time on the radiolabeling efficiency in alkaline solution at room temperature and 90 °C, respectively (method 2). What is interesting in this data is that a decay-corrected radiolabeling efficiency of 99% could be achieved after 10 min heating for a 5 mg ml^{-1} of dextran in alkaline solution. Comparison of the results of two methods reveals that the formation of a ^{68}Ga-dextran complex is more favorable than precipitation of $^{68}Ga(OH)_3$ in alkaline solution. It could be related to the high number

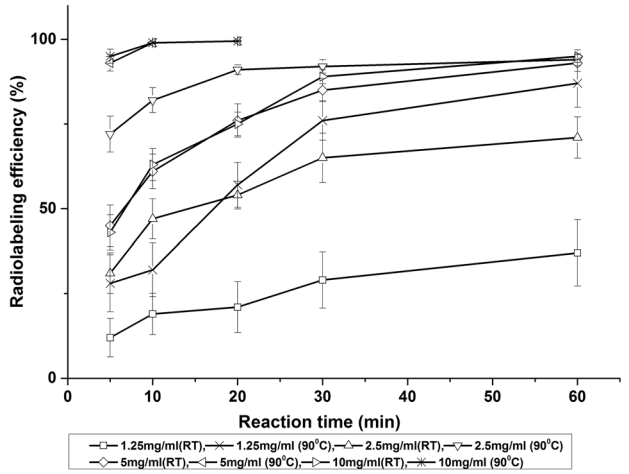

Fig. 3 Radiolabeling efficiency of dextran with ^{68}Ga in alkaline solution (method 2). Each point represents the average of three independent tests

deprotonated hydroxyl groups of dextran in the alkaline solution.

Stability studies in storage solution and toward cysteine and human blood serum

Figure 4 presents the stability profile of ^{68}Ga-dextran solution in the storage solution ($C_{dextran}$ = 5 mg ml^{-1}), in the presence of cysteine ($C_{dextran}/C_{cysteine}$ = 1/100), and human serum. After 2 h of incubation, the radiochemical purity of the radio-complex decreased to approximate 88, 71 and 86% in the storage solution, toward cysteine and human serum, respectively. Although the compound showed a slight instability in the cysteine solution, it was stable enough in human serum to be used in the in vivo studies. Instability of radio-complexes in human serum is mainly related to trans-chelation of the radioisotope to transferrin. Although, transferrin has high binding constant for Ga(III) cations [31]. However, the ^{68}Ga-dextran complex showed a higher stability in human serum than in cysteine solution. Since, the radiolabeled dextran, as a blood-pool radiotracer, shows a long blood circulation profile [6]. The high stability of ^{68}Ga-dextran in human serum could be attributed to the possible poor physical interaction of dextran and transferrin molecules. The same result has also been reported for an ^{188}Re-cysteine conjugated dextran complex [12].

Biodistribution studies

The percent ID g^{-1} of organ values obtained from tissue sampling studies as well as the percent image ROI derived ID g^{-1} values extracted from PET/CT images could be compared in Table 1. There was a suitable correlation

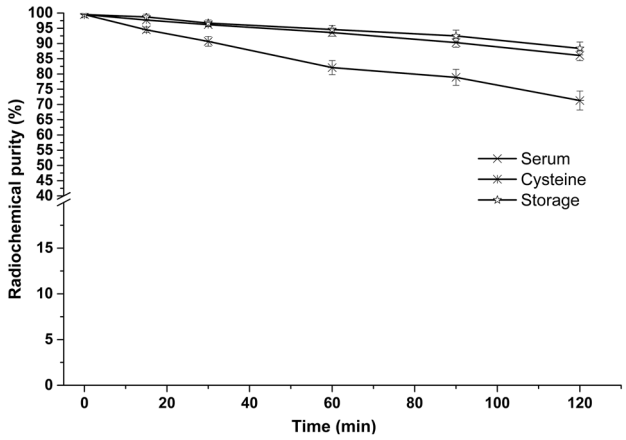

Fig. 4 Stability of ^{68}Ga-dextran in the storage condition and toward cysteine and human serum

between the results of two methods, showing the reliability of ROI derived ID g^{-1} biodistribution study. However, the ROI derived ID g^{-1} of the heart presents the average of ID g^{-1} values of heart tissue and blood inside. The ID g^{-1} of the femur bone is larger than its ROI derived value because the femur samples contained the cartilages too.

Unlike the biodistribution profile of $^{68}GaCl_3$ [32, 33], the largest amount of the injected ^{68}Ga-dextran was accumulated in the lungs at study duration. It could be related to the presence of ^{68}Ga dextran precipitation or cross-linked complex formed in harsh alkaline reaction condition [18]. The other high ID g^{-1} values were for the blood, liver, bladder, kidneys and significant uptakes were observed in the bone, knee joints, and tail fragments. The significant uptake of bone could be attributed to the high affinity of dextran to the bone as it has been used to synthesize dextran-based bone tracers [34].

It is known that Ga(III) ions are bonded to the transferrin as soon as 15 min after administration of any weak Ga(III) complexes such as gallium citrate and gallium chloride solution [31, 35, 36]. Several reports have shown that a small fraction of the injected dose is excreted from renal route and the kidneys to blood ID g^{-1} ratio ranged from 0.18 to 0.43 at 1 h post injection of $^{68}GaCl_3$ [32, 37, 38], whereas in this study, the ^{68}Ga-dextran complex showed a fast excretion profile and a kidney to blood ID g^{-1} ratio of

Table 1 ^{68}Ga-dextran biodistribution in normal rats

Tissue	Time post injection (min)							
	30		60		90		120	
	% Tissue sampling ID g^{-1}	% ROI–derived ID g^{-1}	% Tissue sampling ID g^{-1}	% ROI–derived ID g^{-1}	% Tissue sampling ID g^{-1}	% ROI–derived ID g^{-1}	% Tissue sampling ID g^{-1}	% ROI–derived ID g^{-1}
Blood	1.12 ± 0.20	–	0.71 ± 0.15	–	0.44 ± 0.21	–	0.21 ± 0.06	–
Urine	0.37 ± 0.13	–	–	–	–	–	–	–
Liver	1.17 ± 0.26	1.25	0.61 ± 0.08	0.58	0.31 ± 0.09	0.35	0.17 ± 0.04	0.20
Gall bladder	0.71 ± 0.09	0.93	0.57 ± 0.24	0.79	0.61 ± 0.11	0.74	0.51 ± 0.1	0.67
Spleen	0.5 ± 0.14	0.74	0.39 ± 0.12	0.41	0.29 ± 0.04	0.27	0.13 ± 0.03	0.17
Lung	3.1 ± 0.68	2.8	1.36 ± 0.37	1.74	1.04 ± 0.13	1.01	0.34 ± 0.1	0.49
Heart	0.47 ± 0.32	1.74	0.22 ± 0.19	1.14	0.27 ± 0.14	0.71	0.14 ± 0.09	0.46
Kidneys	0.64 ± 0.27	0.72	0.45 ± 0.1	0.58	0.31 ± 0.09	0.40	0.27 ± 0.12	0.31
Stomach	0.41 ± 0.11	0.35	0.28 ± 0.08	0.26	0.15 ± 0.02	0.19	0.12 ± 0.1	0.14
Intestine, large	0.47 ± 0.06	0.35	0.26 ± 0.11	0.34	0.19 ± 0.07	0.37	0.14 ± −0.03	0.27
Intestine, small	0.27 ± .08	0.34	0.19 ± 0.04	0.25	0.14 ± 0.04	0.25	n.m.	0.18
Bone, femur[a]	0.46 ± 0.1	0.29	0.44 ± 0.11	0.21	0.34 ± 0.11	0.22	0.25 ± 0.07	0.16
Bone, Rib	0.22 ± 0.15	0.33	0.18 ± 0.06	0.24	0.16 ± 0.02	0.15	n.m.	0.11
Brain	0.06 ± .0.07	0.12	0.05 ± 0.03	0.07	n.m.	0.06	n.m.	0.03
Testis	0.21 ± 0.07	0.24	0.12 ± 0.01	0.17	0.1 ± 0.02	0.14	n.m.	0.10
Muscle	0.16 ± 0.09	0.16	0.09 ± 0.05	0.17	0.12 ± 0.01	0.15	n.m.	0.11
Knee	–	0.61	–	0.53	–	0.46	–	0.36

[a] The total femur bones including both sides cartilage were used to measurements

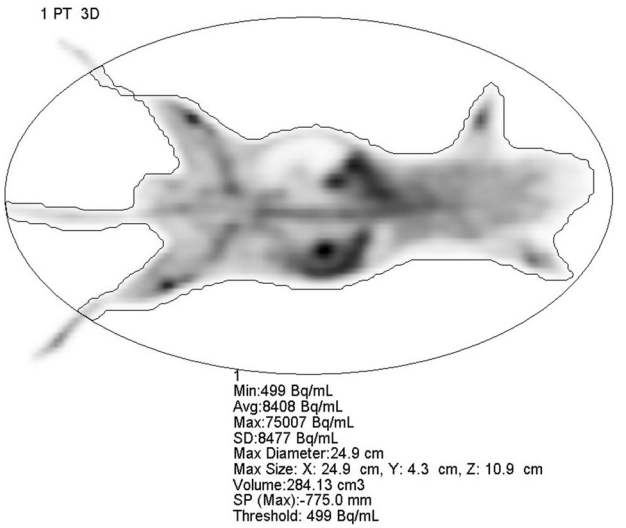

Fig. 5 3D whole body ROI volume and radioactivity concentration of rats

0.63. The fast renal route excretion profile shows that Ga(III) ions mostly present as a chemical form of the ^{68}Ga-dextran complex in the blood circulation. It is notable that the low molecular dextran molecules were eliminated through renal clearance [39].

To determine the uptake and release profile of organs, the total radioactivity within rat's whole-body was determined by multiplying the whole-body volume and average radioactivity concentrations at each study time (Fig. 5). The ratios of the average radioactivity concentration of each organ and the total radioactivity were plotted as a function of time (Fig. 6). At 30 min of post-injection, the highest ratio was for the lung followed by the heart (with blood inside), liver, bladder, kidneys, knee joints and large intestine. Over time, these ratios for the lungs, liver, spleen and heart decreased and for bladder, large intestine and knee joint increased. However, it remained relatively constant for kidneys. The profile outlines that the radio-complex mostly existed in the blood circulation or accumulated in the lungs, liver, and spleen and over time excreted from the body more by the urinary and less by the biliary pathways. The observed increase for knee joints and tail fragments represents the affinity of radio-complex to cartilage tissue and a low release to uptake rate.

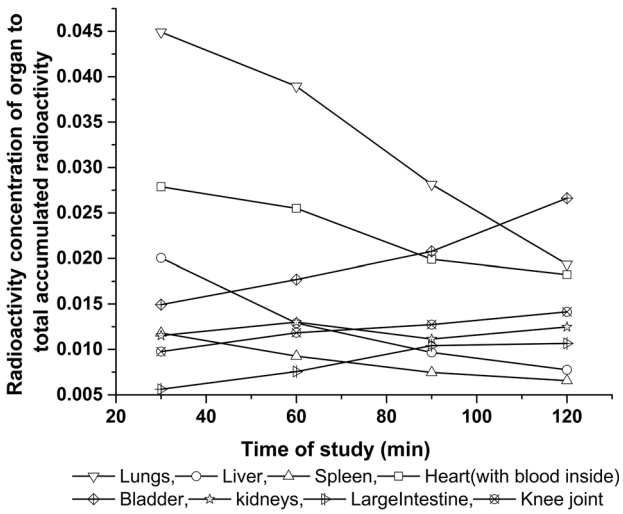

Fig. 6 Radioactivity concentration of organs to total accumulated radioactivity as a function of time

Conclusions

This study set out to determine the possibility of the preparation of ^{68}Ga-dextran as a positron emitter radio-complex. This study has shown that unexpectedly a high radiochemical pure ^{68}Ga-dextran complex was not formed in the acidic HEPES solution even after 1 h heating at 90 °C for a 10 mg ml^{-1} dextran solution. However, a chelator free ^{68}Ga-dextran complex with a radiolabeling efficiency and radiochemical purity of 99% was achieved for a 5 mg ml^{-1} dextran solution and 10 min heating in an alkaline (pH = 9) solution. Generally, ^{68}Ga-dextran presented a lower stability compared to the radioisotopes-DTPA,-MAG$_3$ dextran complexes [14, 15]. However, it was stable enough in human serum for both clinical and research PET imaging applications. The biodistribution data outline a high uptake in the lungs, possibly due to the existence of ^{68}Ga-dextran precipitation or cross-linked complex formed in harsh alkaline condition. The radio-complex showed a more urinary system and a less biliary excretion profile. It is recommended that further study be undertaken using modified dextran derivatives to be labeled in a mild radiolabeling condition.

Acknowledgements This research has been supported by Tehran University of Medical Sciences and Health Services Grant 94-02-58-29793.

References

1. Rahmim A, Zaidi H (2008) PET versus SPECT: strengths, limitations and challenges. Nucl Med Commun 29:193–207
2. Bateman TM (2012) Advantages and disadvantages of PET and SPECT in a busy clinical practice. J Nucl Cardiol 19:3–11
3. Schwaiger M, Wester H-J (2011) How many PET tracers do we need? J Nucl Med 52(Suppl 2):36S–41S
4. Hicks RJ, Hofman MS (2012) Is there still a role for SPECT–CT in oncology in the PET–CT era? Nat Rev Clin Oncol 9:712–720
5. Dilsizian V (2016) Transition from SPECT to PET myocardial perfusion imaging: a desirable change in nuclear cardiology to approach perfection. J Nucl Cardiol 23:337–338
6. Henze E, Robinson GD, Kuhl DE, Schelbert HR (1982) Tc-99 m dextran: a new blood-pool-labeling agent for radionuclide angiocardiography. J Nucl Med 23:348–353

7. Saatchi K, Gelder N, Gershkovich P, Sivak O, Wasan KM, Kainthan RK, Brooks DE, Häfeli UO (2012) Long-circulating non-toxic blood pool imaging agent based on hyperbranched polyglycerols. Int J Pharm 422:418–427
8. Hoffend J, Mier W, Schuhmacher J, Schmidt K, Dimitrakopoulou-Strauss A, Strauss LG, Eisenhut M, Kinscherf R, Haberkorn U (2005) Gallium-68-DOTA-albumin as a PET blood-pool marker: experimental evaluation in vivo. Nucl Med Biol 32:287–292
9. Mathias CJ, Welch MJ, Green MA, Diril H, Meares CF, Gropler RJ, Bergmann SR (1991) In vivo comparison of copper blood-pool agents: potential radiopharmaceuticals for use with copper-62. J Nucl Med 32:475–480
10. Anderson CJ, Rocque PA, Weinheimer CJ, Welch MJ (1993) Evaluation of copper-labeled bifunctional chelate-albumin conjugates for blood pool imaging. Nucl Med Biol 20:461–467
11. Basuli F, Li C, Xu B, Williams M, Wong K, Coble VL, Vasalatiy O, Seidel J, Green MV, Griffiths GL, Choyke PL, Jagoda EM (2015) Synthesis of fluorine-18 radio-labeled serum albumins for PET blood pool imaging. Nucl Med Biol 42:219–225
12. Du J, Marquez M, Hiltunen J, Nilsson S, Holmberg AR (2000) Radiolabeling of dextran with rhenium-188. Appl Radiat Isot 53:443–448
13. Pirmettis I, Arano Y, Tsotakos T, Okada K, Yamaguchi A, Uehara T, Morais M, Correia JDG, Santos I, Martins M, Pereira S, Triantis C, Kyprianidou P, Pelecanou M, Papadopoulos M (2012) New $^{99m}Tc(CO)_3$ mannosylated dextran bearing S-derivatized cysteine chelator for sentinel lymph node detection. Mol Pharm 9:1681–1692
14. Hoh CK, Wallace AM, Vera DR (2003) Preclinical studies of [^{99m}Tc] DTPA-mannosyl-dextran. Nucl Med Biol 30:457–464
15. Vera DR, Wallace AM, Hoh CK, Mattrey RF (2001) A synthetic macromolecule for sentinel node detection: ^{99m}Tc-DTPA-mannosyl-dextran. J Nucl Med 42:951–959
16. Vera DR, Wallace AM, Hoh CK (2001) [99mTc] MAG3-mannosyl-dextran: a receptor-binding radiopharmaceutical for sentinel node detection. Nucl Med Biol 28:493–498
17. Norkus E, Vaičiūnien J, Vuorinen T, Heikkilä M (2002) Interaction of Cu(II) with dextran in alkaline solutions. Carbohydr Polym 50:159–164
18. Somsook E, Hinsin D, Buakhrong P, Teanchai R, Mophan N, Pohmakotr M, Shiowatana J (2005) Interactions between iron(III) and sucrose, dextran, or starch in complexes. Carbohydr Polym 61:281–287
19. Gyurcsik B, Nagy L (2000) Carbohydrates as ligands: coordination equilibria and structure of the metal complexes. Coord Chem Rev 203:81–149
20. Rösch F (2013) ^{68}Ge/^{68}Ga generators and ^{68}Ga radiopharmaceutical chemistry on their way into a new century. J Postgrad Med Educ Res 47:18–25
21. Velikyan I (2013) Prospective of ^{68}Ga-radiopharmaceutical development. Theranostics 4:47–80
22. Vorster M, Maes A, Van deWiele C, Sathekge M (2013) Gallium-68: a systematic review of its nononcological applications. Nucl Med Commun 34:834–854
23. Khan MU, Khan S, El-Refaie S, Win Z, Rubello D, Al-Nahhas A (2009) Clinical indications for gallium-68 positron emission tomography imaging. Eur J Surg Oncol 35:561–567
24. Rösch F (2013) Past, present and future of ^{68}Ge/^{68}Ga generators. Appl Radiat Isot 76:24–30
25. Bernstein LR (1998) Mechanisms of therapeutic activity for gallium. Pharmacol Rev 50:665–682
26. Peng M, Li H, Luo Z, Kong J, Wan Y, Zheng L, Zhang Q, Niu H, Vermorken A, Van de Ven W, Chen C, Zhang X, Li F, Guo L, Cui Y (2015) Dextran-coated superparamagnetic nanoparticles as potential cancer drug carriers in vivo. Nanoscale 7:11155–11162
27. Yu M, Huang S, Yu KJ, Clyne AM (2012) Dextran and polymer polyethylene glycol (PEG) coating reduce both 5 and 30 nm iron oxide nanoparticle cytotoxicity in 2D and 3D cell culture. Int J Mol Sci 13:5554–5570
28. Tassa C, Shaw SY, Weissleder R (2011) Dextran-coated iron oxide nanoparticles: a versatile platform for targeted molecular imaging, molecular diagnostics, and therapy. Acc Chem Res 44:842–852
29. Mirzaei A, Jalilian AR, Shabani G, Fakhari A, Akhlaghi M, Beiki D (2016) Development of ^{68}Ga ethyl cysteinate dimer for PET studies. J Radioanal Nucl Chem 307:725–732
30. Saito AI, Li JG, Liu C, Olivier KR, Dempsey JF (2009) Accurate heterogeneous dose calculation for lung cancer patients without high-resolution CT densities. J Appl Clin Med Phys 10:2847
31. Harris WR, Pecoraro VL (1983) Thermodynamic binding constants for gallium transferrin. Biochemistry 22:292–299
32. Steinberg JD, Raju A, Chandrasekharan P, Yang CT, Khoo K, Abastado JP, Robins EG, Townsend DW (2014) Negative contrast Cerenkov luminescence imaging of blood vessels in a tumor mouse model using [^{68}Ga] gallium chloride. EJNMMI Res 4:15–26
33. Velikyan I, Xu H, Nair M, Hall H (2012) Robust labeling and comparative preclinical characterization of DOTA-TOC and DOTA-TATE. Nucl Med Biol 39:628–639
34. Tanaka H, Yamaguchi S, Jo J, Aoki I, Tabata Y, Takahashi T (2014) Synthesis of a dextran-based bone tracer for in vivo magnetic resonance and optical imaging by two orthogonal coupling reactions. RSC Adv 4:7561–7565
35. Tsan MF, Scheffel U (1986) Mechanism of gallium-67 accumulation in tumors. J Nucl Med 27:1215–1219
36. Vallabhajosula SR, Harwig JF, Wolf W (1981) The mechanism of tumor localization of gallium-67 citrate: role of transferrin binding and effect of tumor pH. Int J Nucl Med Biol 8:363–370
37. Bhatt J, Mukherjee A, Korde A, Kumar M, Sarma HD, Dash A (2016) Radiolabeling and preliminary evaluation of Ga-68 labeled NODAGA-ubiquicidin fragments for prospective infection imaging. Mol Imaging Biol 18:1–9. doi:10.1007/s11307-016-0983-4
38. Velikyan I, Antoni G, Sörensen J, Estrada S (2013) Organ biodistribution of Germanium-68 in rat in the presence and absence of [^{68}Ga] Ga-DOTA-TOC for the extrapolation to the human organ and whole-body radiation dosimetry. Am J Nucl Med Mol Imaging 3:154–165
39. Maia J, Evangelista MB, Gil H, Ferreira L (2014) Dextran-based materials for biomedical applications. Res Signpost 37661:31–53